

# ALLFLIGHT: HELICOPTER PILOT ASSISTANCE IN ALL PHASES OF FLIGHT

Robin Lantzsch<sup>1</sup>, Steffen Greiser<sup>1</sup>, Jens Wolfram<sup>1</sup>, Johannes Wartmann<sup>1</sup>, Mario Müllhäuser<sup>1</sup>  
[robin.lantzsch@dlr.de](mailto:robin.lantzsch@dlr.de), [steffen.greiser@dlr.de](mailto:steffen.greiser@dlr.de), [jens.wolfram@dlr.de](mailto:jens.wolfram@dlr.de), [johannes.wartmann@dlr.de](mailto:johannes.wartmann@dlr.de), [mario.muellhaeuser@dlr.de](mailto:mario.muellhaeuser@dlr.de)  
Thomas Lüken<sup>2</sup>, Hans-Ullrich Döhler<sup>2</sup>, Niklas Peinecke<sup>2</sup>  
[thomas.lueken@dlr.de](mailto:thomas.lueken@dlr.de), [ulli.doehler@dlr.de](mailto:ulli.doehler@dlr.de), [niklas.peinecke@dlr.de](mailto:niklas.peinecke@dlr.de)

<sup>1</sup>Institute of Flight Systems, <sup>2</sup>Institute of Flight Guidance  
German Aerospace Center (DLR)  
Braunschweig, Germany

## ABSTRACT

The DLR internal project ALLFlight (**Assisted Low Level Flight** and Landing on Unprepared Landing Sites) deals with the development of a helicopter pilot assistance system, which assists the pilot through all phases of flight. The system covers takeoff, intermediate low level flight and landing on unprepared sites in the presence of obstacles and in a degraded visual environment. The paper describes the implementation of the full scale pilot assistance system into DLR's Active Control Technology / Flying Helicopter Simulator (ACT/FHS) testbed. The unique ALLFlight full scale pilot assistance system gives the research establishment the opportunity to test the whole chain from sensors, via the data fusion and trajectory planning including active inceptors to modern flight control techniques in real time in the real world during flight tests.

## 1 INTRODUCTION

Compared to fixed-wing aircraft flying a helicopter is still relatively unsafe. The number of accidents per 100,000 flight hours of about 4.9 [1] in 2007 is still too high (for fixed-wing commercial aircraft it is 0.139 accidents per 100,000 flight hour [2]). Main contributing factors to the high numbers are pilot misjudgments and the resulting actions [3] due to high workload and bad weather conditions. New ways to assist the pilots in flying the helicopter should be developed to raise the level of safety in flying helicopters.

In the framework of ALLFlight sensors which are able to see through the atmosphere in darkness as well as under bad weather conditions are integrated on DLR's research helicopter ACT/FHS. The sensed data will be fused to one three-dimensional terrain scenery, which first of all can be presented to the pilot via a helmeted mounted display (HMD). Secondly, the terrain data are used for all trajectory planning processes. The respective elevation map is generated from databases and the online fusion process. The planned unsteady curved trajectory can be used to guide the pilot via e.g. a tunnel in the sky on his HMD or to fly automatically on the planned path. To give the pilot the possibility to fly on this path modern flight control laws with different levels of automation can be used. The corresponding level can be adjusted manually or automatically with respect to the outside conditions (e.g. the usable cue environment [28]). The interaction with the flight control system is handled by the pilot via active inceptors. One extreme of this research is the fully automatic flight and landing of a manned helicopter in a confined area.

ALLFlight is not the first project aiming to reduce accident rates by reducing pilot workload. In the last years several projects dealt with the development of pilot assistance systems.

During the project PhLASH (Photographic Landing Augmentation System) the USAF Laboratory Rapid Reaction Team successfully integrated and tested a science and technology solution. This "see and remember" system shall reduce aircraft accidents resulting from the loss of visual cues during takeoffs and landings in dusty conditions [4, 5]. The solution is "a combination of an electro-optical sensor and infrared strobe lights which images and geo-registers (matches the image to a coordinate on the earth's surface) the ground prior to landing in brownout conditions".

The project LandSafe™, an Optical Air Data Systems, LLC program, attempted to introduce a new solution to help helicopters in navigating and landing safely in degraded visual environments, especially brownout conditions. The LandSafe solution incorporates commercial off-the-shelf fiber optic laser technology to "sense through" particulate matter such as dust, snow, rain, smoke or fog while providing altitude, ground speed and airspeed information to the flight crew [6].

The Sandblaster program is an initiative lead by the US Defense Advanced Research Projects Agency (DARPA) [7]. It involves the participation of the US Army, Air Force and Marines to varying degrees. It integrates a radar as image sensor. Then a database fuses the generated images with stored images. To restore the pilot's lost visual cues an advanced three-dimensional synthetic vision system is used. An agile automatic flight control system tailored for low-speed operations during landing,

offers the pilot the possibility to let the helicopter land automatically.

Another part of pilot assistance is dealing with control law design. The project ACTIME (Active Control Technology for Improved Mission Effectiveness) of Eurocopter dealt with control law development to increase the handling qualities level to 1. One output of the project was that the control laws used are only one part of the pilot assistance architecture that would be required to reach this goal. Using the haptic feedback channel of a pilot the project NRTC/RITA worked with a 3-axis active sidestick (1999-2000) as predecessor of HACT [8]. The project HACT (Helicopter Active Control Technology), a US Army Aviation Applied Technologies Directorate funded program, used right hand and left hand sidesticks [9] to control the aircraft and a flight control system to enhance mission effectiveness and all-weather capabilities. Advanced control law design is also used on the RASCAL, a JUH-60A Black Hawk helicopter based at the U.S. Army Aeroflightdynamics Directorate in Moffett Field, CA. This work uses the classical explicit model following control law design with a frequency-dependent feedback controller. The controller consists e.g. for the lateral axis of a cascade structure (a roll control inner loop and a lateral speed outer loop), a washout filter for higher reactivity and a yaw crossfeed to reduce uncommanded off-axis responses. For control law design a high-order, linearized model of the UH-60 was used. Flight tests have been performed to validate the control laws quantitatively using frequency sweeps and qualitatively using ADS-33 mission task elements [10].

The UH-60M upgrade program was using active inceptors in a conventional long pole configuration. This system was tested and optimized on the RASCAL. This project is described in more detail in [11].

The focus on pilot assistance was set in the DLR project PAVE (Pilot Assistance in the Vicinity of Helipads) to develop an assistance system to land on helipads. Here, path planning and design of the visual displays were in the primary focus [12]. Similar work was done in Eurocopter's PILAS (Pilot Assistance System) project, which developed a planning and guidance system for helicopter emergency medical service (HEMS) missions. The project used advanced displays to display the planned paths and a 4-axis autopilot flying them automatically.

In [13] an analogous work to the ALLFlight project is presented using a full scale unmanned helicopter: the Boeing Unmanned Little Bird. The Little Bird flies automatically through unmapped terrain and finds a landing zone, all without any human control input.

All of these projects have in common that they deal only with one part of the overall assistance or demonstrate the function without human interaction on unmanned helicopters. ALLFlight uses lessons learned from previous projects (e.g. ACTIME), in that it combines several options simultaneously for pilot assistance, whereas the other projects used only a single one. ALLFlight is the first project which uses a manned in-flight simulator and covers all fields of pilot assistance: acquiring and processing sensor data, trajectory planning, modifying the flight dynamics, using active inceptors, and showing the necessary information to a head down or head up display. The paper describes the set-up of this full scale pilot assistance test environment. First preliminary results are also shown.

## 2 THE ALLFLIGHT PROJECT

ALLFlight is a DLR internally funded project. It was started in 2008 and will be finished by the end of 2012. The objective of ALLFlight is to achieve a safe and effective 24-hours all-weather operation capability under the above mentioned conditions by providing the pilot with an optimal combination of assistance subsystems. This system reduces his workload and increases both situational and mission awareness, by means of advanced cueing (visual and tactile) and advanced control augmentation. An extreme of this development is the fully automatic flight and landing of a manned helicopter in a confined area.

Figure 1 describes the system architecture of the ALLFlight full scale pilot assistance test environment. It consists of 6 basic parts: sensors, 3D-model sensor data fusion, trajectory planning, model based control, active inceptors, and the head down display (HDD) as well as the helmet mounted display (HMD). These parts are summarized shortly in the following paragraphs and are described more extensively in the next sections.

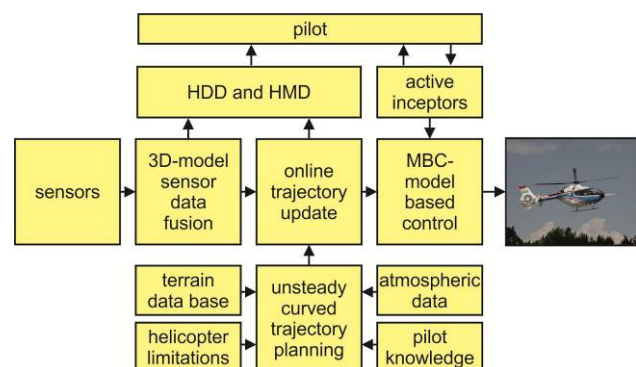


**Figure 1. ALLFlight system architecture**

**SENSORS:** For the 3D environmental model generation the DLR research helicopter ACT/FHS is upgraded with different sensors (laser, radar,

infrared) to acquire data from the outside world (see Table 1 for more details on the sensors used).

**3D-MODEL SENSOR DATA FUSION:** The data of the different imaging sensors are fused to create a digital map (3D terrain model). Based on this digital map, a trajectory planning algorithm is applied for the described flight phases. Both, map generation and trajectory planning are executed in real-time. It is possible to plan curved and unsteady trajectories (in space and time) for all phases of the helicopter flight (takeoff, low level flight, landing) under all conditions (day, night, degraded vision).

**TRAJECTORY PLANNING:** The trajectory generation considers the cognitive pilot's decision processes as well as the atmospheric conditions and the flight mechanical limits of the helicopter. At least a subset of the pilot's cognitive processes is represented by the results of a pilot questionnaire. This questionnaire covers specific requirements usually considered by the pilots while performing their missions. Thus it is assured that the calculated trajectories can be flown by the aircraft and are accepted by the helicopter pilots. Nevertheless, the pilot will be able to affect the planned trajectories by changing the parameters of the planning algorithm. Of course, an autopilot can be used for fully automatic flight, but, further on, the pilot still has the possibility to control the helicopter indirectly by controlling the resulting trajectories. In a preplanning process the unsteady curved trajectory will be planned with respect to a digital elevation map. During flight the trajectory will be updated online in case of a newly detected obstacle.

**MBC – MODEL BASED CONTROL:** The latest handling qualities insights drive the development and maturing of the relevant assistance systems (augmentation, visual, and haptic support) and their coalescence to allow the pilot an intuitive following of the generated trajectories or surfaces depending on the present flight phase and environmental conditions. The integration of the whole system together with all relevant flight tests will be performed on the ACT/FHS research helicopter.

**ACTIVE INCEPTORS:** The ACT/FHS has been equipped with two active sidesticks, for cyclic, collective, and optionally for yaw control. The use of active inceptors opens an additional feedback path to the pilot, the so called haptic feedback. The ALLFlight project will integrate this channel into the man-machine interface.

**HDD and HMD:** As a first step for visualization the ALLFlight project will use the conventional HDD technology to present visual cues / information to the pilot. At the end of this overall project DLR will also work in the field of 3D-conformal visualization on a wide field of view HMD system. One main aspect of using an HMD is the possibility to increase the

situational awareness of the pilot during low level flights and landings. The integration into the ACT/FHS is in progress and will be finished by mid-2012.

The ALLFlight full scale pilot assistance test environment makes it possible to test simultaneously all the aforementioned pilot assistance subsystems in real time under real conditions during flight tests. The next chapter provides a short introduction of the ACT/FHS.

### 3 ACT/FHS THE FLIGHT TEST VEHICLE

The ACT/FHS research helicopter (Figure 2) is based on a Eurocopter EC135, which is a light, twin engine helicopter with a bearingless main rotor and a fenestron. The mechanical controls were replaced by a full authority fly-by-wire/fly-by-light primary control system [14].



**Figure 2. Active Control Technology/Flying Helicopter Simulator (ACT/FHS)**

Figure 3 shows the overall system architecture of the ACT/FHS.

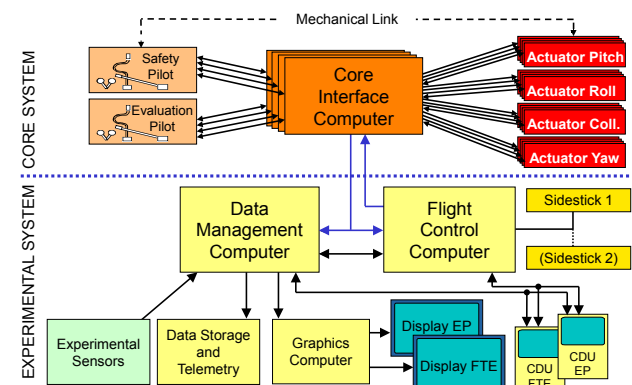


**Figure 3. ACT/FHS system architecture**

The core system (above the blue dotted line) meets the high civil aviation safety requirements with a catastrophic failure probability of  $10^{-9}$  per flight hour. All components are 4 times redundant (quadruplex). The connections between the pilot controls and the core interface computer are by wire and between the core interface computer and the actuator units by

light. In the experimental mode, the evaluation pilot's controls are fed through the experimental system (under the blue dotted line) and after processing back to the core system with full authority. Safe operation is guaranteed by the safety pilot flying hands on to monitor the actuator displacements. The safety pilot's controls move synchronously with the actuators due to the mechanical link between them. In case of control drifts or runaways the safety pilot is alerted to take over the control by pushing a button or force-overriding the experimental control input.

The experimental system is designed only simple, which provides the high flexibility that is required for research activities. The adaptable system allows different users a fast change of software or hardware configurations. On the FCC (flight control computer) the user can implement his applications. Overall data handling, recording and telemetry is done by the separate DMC (data management computer). Via the CDU (control and display unit) the flight test engineer (FTE) or the evaluation pilot (EP) can adjust control system parameters or control sensor and system status. A telemetry downlink allows the ground crew to monitor most of the flight data, controller states, and configuration parameters. The ground crew is responsible to observe any occurrence of structural vibrations and to assist the flight crew in performing the experiments.

#### 4 SENSORS

Current development of enhanced vision systems in aviation is mainly triggered by the availability of imaging sensors that are able to see through the atmosphere in darkness as well as under bad weather conditions. Up to now, IR camera technology (3-5 or 8-12 microns) provides the most mature sensor for such applications. The high maturity of IR cameras is mainly a result of a long lasting development in numerous military applications, where IR technology was mostly used as a night vision sensor. The relatively low cost of IR cameras especially of the modern uncooled bolometer type is their second advantage. However, as shown in Figure 4, millimeter waves (mmW) are able to penetrate a foggy atmosphere even better than IR radiation.

Therefore, in most applications requiring looking through fog, mmW radar systems are used. These systems work usually within the three main windows at 35, 77 and 94 GHz. Although numerous ranging sensors exist for automotive applications where distance measuring and automatic distance control between succeeding cars are the objectives, there are only few mmW radar systems available for airborne applications.

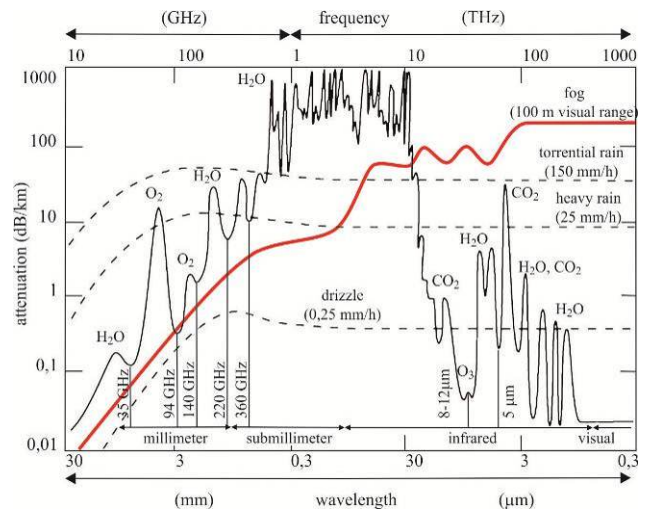


**Figure 4. Attenuation of the atmosphere (in dB/km) for different visual conditions depends on wavelength (in mm or micron). Rule of thumb: the longer the wavelength - the lower the attenuation [15], red thick line fog, 100 m visibility**

The current challenge to help helicopter crews under very different degraded visual situations like brownout, whiteout, darkness, fog, and snow will hardly be solved by installing a single sensor only. For such a variety of different visual degradations an intelligent combination of a set of different imaging sensors will be indispensable. The sensor types and models for ALLFlight's sensor suite were chosen based on availability, maturity, and price (see Table 1). The approach was to use commercial off-the-shelf (COTS) products which at most needed smaller adaptations to be integrated into the project.

Together with Eurocopter Germany, DLR developed a special equipment carrier beam to install all sensors under the forward cross tube of the landing skid (Figure 5). In addition, the helicopter was equipped with a higher landing skid to achieve the necessary ground clearance for the sensors in unprepared landing sites. In cooperation with the German certification authorities an extensive flight test program was conducted in mid-2011. Up to now the electrical certification of the radar system is not finalized. The first flight test with the radar system is scheduled for late 2012.

All these sensors are connected to the experimental system of the ACT/FHS. The flight states (e.g. position, attitude, etc.) are provided from the data management computer (DMC). The acquired data from the sensors are fed into the sensor co-computer SCC, which is part of the system architecture. For acquisition, recording, analysis, and visualization of sensor data a specialized distributed software system was designed and implemented. The software system, which runs

under Microsoft's Windows XP operating system, was developed in C/C++.

**Table 1. Overview of the sensors used**

			
HELLAS Ladar	AI-130 radar	EVS-1000 infrared	Camera TV
1.5 micron	35 GHz pulse radar	8-12 micron	visible spectrum
FOV 31,5°x32°	FOV 180°x110°	FOV 53°x40°	FOV 53°x40°
95x200 pixels max.	beam width 2,4°x1,8° range 1000 m	320x240 pixels	768x494 pixels
range res. 0.6m	range res. 1.8 m	NETD 0.2K	sensitivity 0.1 lux
scan freq. 2 Hz	scan time 1.8 sec for FOV 30°x21°		
LAN-Interface	LAN-Interface	RS-170 Interface	RS-170 Interface

FOV... Field of View; NETD... Noise Equivalent Temperature Difference



**Figure 5. Integrated sensor suite close up**

## 5 SENSOR DATA FUSION

One of the central tasks of ALLFlight is to make the data from multiple sensors available to the pilot. For this, sensor data fusion takes place at different stages of the information processing.

One part of the data fusion pipe is a given database of elevation data, for example, from SRTM (shuttle radar topography mission). Incoming data from radar and Ladar are time stamped, mapped to ground references, and then compared to the existing ground information. Time stamping is essential to track whether the return is part of a moving obstacle,

and also in cases where the data become outdated and are to be discarded later.

Based on the classification algorithm, the measured points are either assigned to the ground, previously unrecognized buildings or other obstacles, or discarded as errors. If returns are ground points the data are added to the ground information. For obstacle points it is decided based on history records if they belong to a moving (even flying) obstacle or if their position is fixed. Obstacle points are grouped into coherent objects described by their bounding boxes. In case of a moving object a motion vector can be estimated.

Figure 6 illustrates a conventional TV camera image, which has been recorded during a flight test in the vicinity of the Braunschweig airport. Figure 7, Figure 8 and Figure 9 give an idea about different methods of displaying the results of the obstacle/ground separation algorithms.



**Figure 6. TV image of the vicinity of an apron including a telemetry tower**

Figure 7 displays measured points as part of the terrain. Each point is integrated as an elevation value, thus obstacles appear as smooth hills. It is not possible to recognize advanced form cues.

Figure 8 presents the measured points as columns elevated from the terrain looking much like skyscrapers in Manhattan. The algorithm groups points to a regular 5x5 m grid. Linear obstacles appear as collections of columns (lattice fence effect). In contrast to Figure 7, some limited form cues can be recognized. Figure 9 depicts the measured points as connected cubes of varying size. A separation from ground is possible. The obstacles appear as raw estimates of actual shapes, thus poles, cranes, power lines, etc. can be identified and give an advanced form cue.

In the scope of a human factors investigation, these different display variants have been presented to a number of civil and military pilots to find out the best

way to represent the outside situation on a helmet mounted display [16].

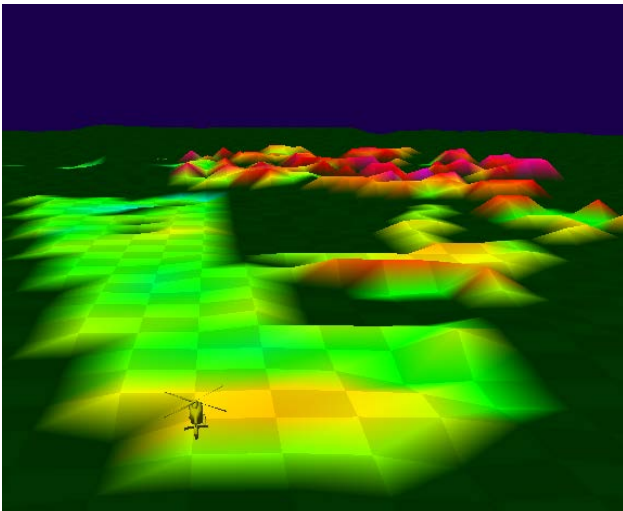


Figure 7. Display variant "Terrain"

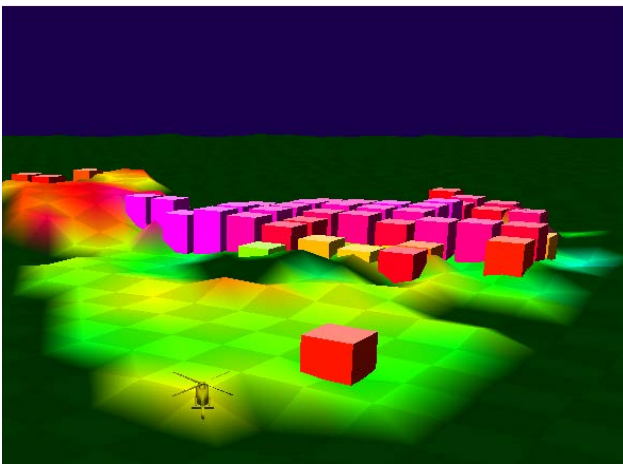


Figure 8. Display variant "Manhattan"

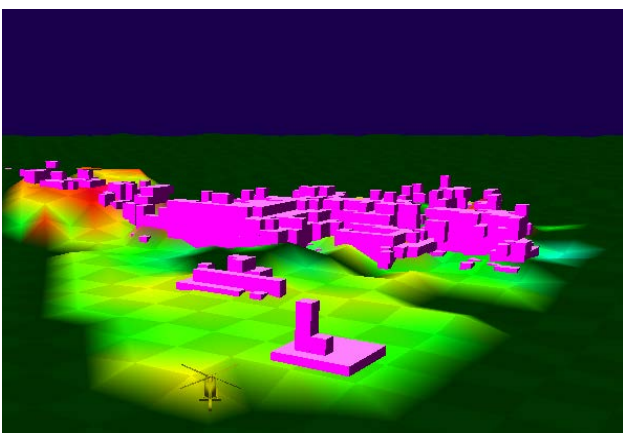


Figure 9. Display variant "Octree"

Regarding the detection of static or moving objects on image-based sensor data (TV, IR, etc.), feature extraction algorithms reduce the incoming flood of data in a first step. The detection of moving objects requires the detection of the same object in a

number of successive frames. The software architecture of the acquisition and recording processes allows a direct memory access of the last acquired number of frames instantaneously. Moving objects are not part of the produced database and are handled separately as an independent data flow. In contrast to the imaging sensors, Ladar- and mmW-Radar data represent 3D geo-referenced measured points, but with a lower data rate.

Further development of fusion algorithms will be a major research topic at DLR for the next few years. Comparison of the ICx radar with the HELLAS sensor and integration of IR data into the fusion will be the next step in the process. The usage of the outcome of the data fusion algorithm, the digital elevation map, by the trajectory planning is described in the next chapter.

## 6 TRAJECTORY PLANNING

This section summarizes the design concept and the methodology to assist helicopter pilots during flight path planning. In general, the planning task depends on the mission or mission element and therefore has a high maneuver complexity. The goal for ALLFlight is to compute unsteady and curved flight paths accounting for helicopter limitations, obstacles, terrain, and pilot preferences. Finally, landing and touchdown should be demonstrated using online data acquisition and online path planning.

### 6.1 Conceptual design

In ALLFlight path planning is subdivided into local and global path planning. The local planner is just a reactionary planning aid accounting for near field obstacles which might be hit in the next few seconds. If there is more time left, global flight path planning is preferred to replan the flight path. In the following, global planning and the ideas as well as the current status of the global flight path planning are presented. The global planner computes a three-dimensional flight path which accounts at least for the provided airspace restrictions. Optionally, other limitations could be taken into account, such as helicopter limits. The mission is characterized by the landing point and if necessary by additional waypoints. The sequence of the waypoints is defined by the pilot, so that the general motion planning problem [17] is easily reduced to a shortest path problem. Therefore, it is not necessary to compute the optimal connection between the waypoints since that is already defined.

However, the planned flight path consists of at least three flight phases which are analyzed by different planning algorithms. These phases are takeoff, enroute, and landing. Not only the mission is an important input but also the sensor information, helicopter limitations, and the pilot's cognitive

processes. The sensor information gives a digital map that is stored in shared memory and can be easily accessed by interface software. The helicopter limitations as well as the pilot's cognitive processes are realized as knowledge-based algorithms.

## 6.2 Helicopter limitations and the pilot's cognitive processes

In general, the limitations given in the flight manual are defined by charts depending on environmental conditions such as outer air temperature or pressure. These limitations define upper bounds or recommendations. Within the ALLFlight project, the values defined by the EC135 are used. These are:

- Maximum rate of climb
- Maximum continuous power
- Maximum velocity
- Height-velocity diagram

As mentioned before, the pilot's cognitive processes are also considered. Since these processes vary between pilots, the individual expectations for the planned flight path will also vary. To reduce the gap between expectation and computational solution, at least a subset of the overall pilot requirements which might be raised for the path planning algorithms are covered by survey data. The survey was performed as interview for takeoff and enroute (2009/2010) and was sent by postal mail for landing (2007/2008). Compared to the interview the postal dispatch has more outliers so that we recommend using first an interview and then the postal dispatch to reduce the uncertainty for particular questions if necessary. However, up to now takeoff and enroute count 68 and landing counts 71 participants. Their respective background is depicted in Figure 10.

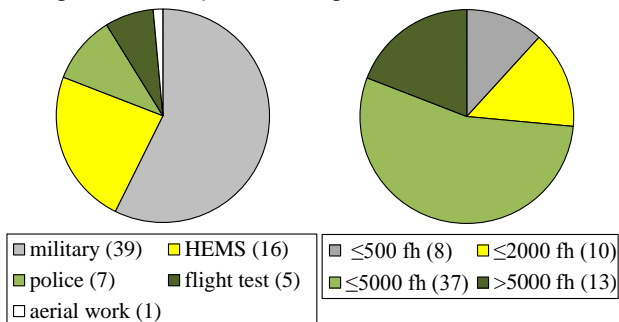


**Figure 10. Takeoff and enroute interview - pilots' background (number of pilots)**

29 of the 68 pilots work in a civil field and 39 pilots are military personnel. The military pilots typically fly SAR (search and rescue) as well as training and instructor flights in military school. The pie chart on the right in Figure 10 shows the flight experience. The pilots' mean flight experience is 3738 flight hours (fh) as pilot in command ranging from pilots who just earned their wings with 100 flight hours to

experienced pilots with more than 11000 flight hours. The average age of the pilots questioned is 43 years with a maximum of 58 and a minimum of 24 years. The group of the participants is well mixed between military and civil pilots as well as experienced and inexperienced pilots. This reflects well the overall helicopter community. Only single engine operations and the general aviation sectors are not well represented.

The helicopter pilots were asked for different planning-relevant constraints. Some of these constraints are:

- preferred true airspeed
- preferred rate of climb
- horizontal and vertical clearance
- accepted wind conditions

In addition the typical standard operating procedures are also analyzed (e.g. reasons to fly vertical or CAT-A takeoff). This gives a first overview of the constraints and maneuvers used for path planning and their dependence on the individual pilot. Based on the gathered data, a pilot classification is computed using the method described in [19]. An overview of the algorithm is shown in Figure 11.

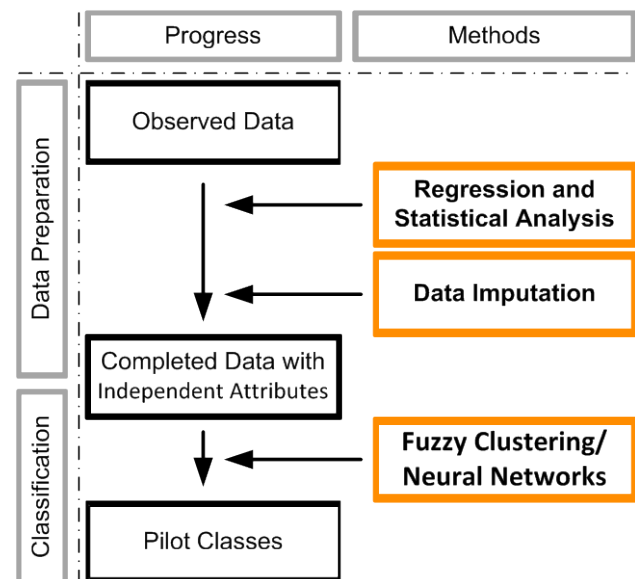


**Figure 11. Algorithm for pilot classification using survey data**

This tool imputes missing data and reduces the database so that only independent requirements without outliers are used for classification. The dependent variables are identified by correlation analysis and then modeled by regression analysis. The data imputation computes estimates of the missing data using the methods proposed in [19, 20, 21]. A cost function finally suggests the probably best imputed database. After data preprocessing, the tool finally calculates the pilot classes by means of fuzzy clustering or neural networks. Again, each

classification result from the different methods is compared to one another by cost function values so that a proper classification result can be selected. Up to now, this tool was used to classify the individual constraints used for takeoff and is currently applied to enroute data.

Finally, each pilot has a degree of membership to every computed pilot class. For takeoff 63 of the 68 pilots are used for clustering. There are 7 attributes which can be categorized into safety margins, wind conditions, and rate of climb. The resulting pilot classes are shown in Figure 12.

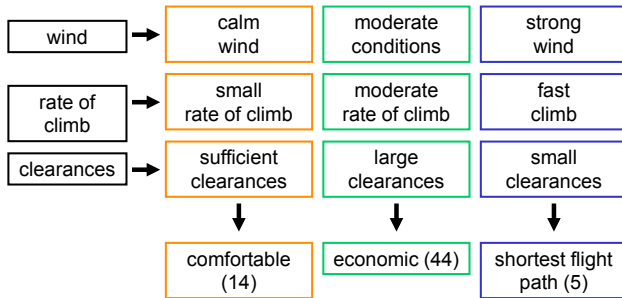


**Figure 12. Results from pilot classification for takeoff**

These classes are represented by specific numerical values which are used as constraints for path planning. Selecting the comfortable class for instance would lead to constraints which result in a flight path that is more smooth, has lower velocity and smaller crosswind components.

### 6.3 Path planning algorithms

The trajectory planning utilizes the user-defined waypoints, sensor information, helicopter limitations, and the pilot's class. This are all input data to compute feasible flight paths. These flight paths are computed based on the A\* [22] and D\*-Lite [23] algorithms which are well-established for motion planning problems [17]. Both methods utilize a graph representing the free configuration space. Based on the graph, the A\* or D\*-Lite algorithm computes an optimal path in accordance with the heuristic. The D\* is used for enroute only, since D\* planning in a three-dimensional space together with the airspeed is less computationally expensive as it would be using the A\* algorithm. Takeoff and landing are reduced to a two-dimensional problem since the respective profiles are known from the flight manual, flight test data, and the survey. Both algorithms make use of cost functions to decide which path is probably best. In general, the cost functions consider at least the kinematics and (filtered) wind conditions to compute the costs.

The computed path is then postprocessed by B-splines or Bezier splines to obtain a smooth flight path. The interpolation effect of spline curves may

yield paths that collide with an obstacle. To avoid this, the interpolation effect is already taken into account during the above mentioned planning.

The planning algorithms are divided in three planning stages (takeoff, enroute, and landing). The next figures show for each planning step one example. During the planning process the takeoff and the landing calculation will be performed first. Afterwards the takeoff climbout point (CP) and the approach entry point will be transferred to the enroute algorithm as start and end point of the enroute phase.

#### 6.3.1 Takeoff

By means of the SP (start point) and TDP (takeoff decision point) an initial takeoff profile is calculated regarding power settings and state constraints. The initial takeoff profile is proved not to crash with any obstacle, but there is no planning algorithm used which avoids obstacles. The position of the TDP and the specifications from the flight manual are used to compute a three-dimensional surface. Within that surface, the unobstructed takeoff trajectory is planned. One takeoff with constant slope is shown in Figure 13. Currently, the planning algorithm for the normal takeoff is prepared for implementation on the ACT/FHS.

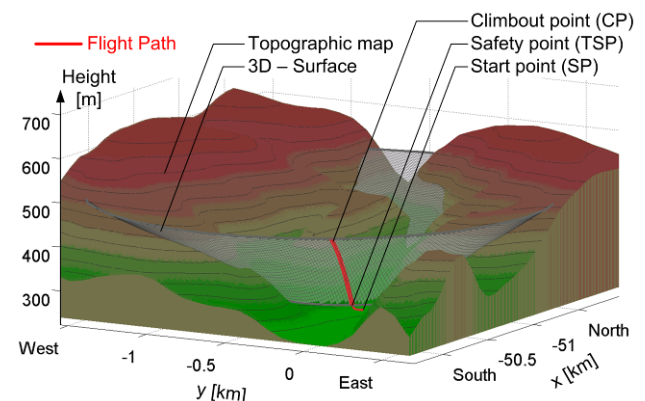


**Figure 13. Planned flight path for takeoff with constant slope**

#### 6.3.2 Landing

The approach planning is currently prepared for flight testing. The level flight at constant altitude, together with a single angle approach, specifies a three-dimensional surface similar to the takeoff profile. Unlike for takeoff, the slope is constant for the whole approach trajectory from level flight to hover [24]. A standard approach uses an air-path inclination angle of between  $-8^\circ$  and  $-12^\circ$  starting at approximately 300ft above the helipad elevation (AHE) with the recommended approach speed of 60 kts indicated airspeed – IAS. The rate of descent



and longitudinal and lateral cyclic, pedal and collective input:

$$u = (\delta_x, \delta_y, \delta_p, \dot{\delta}_0)^T$$

The derivative of the collective control  $\dot{\delta}_0$  in the input vector and the collective control in the state vector result from the equivalent formulation of the inflow dynamics. The whole identification process can be found in [25].

While offline simulation and feedback controller design use identified 11-DoF models, 9-DoF models on the basis of the 11-DoF models discarding the lead-lag dipoles are used for feedforward controller development. Figure 17 shows the comparison of measured and simulated roll accelerations due to lateral input in time domain.

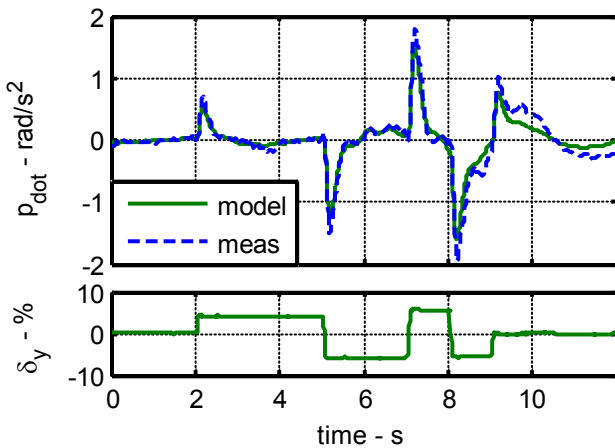


Figure 17. Time domain comparison for roll acceleration due to lateral cyclic input

## 7.2 Command Model

The command model is the part of the model based control that determines the general behavior of the aircraft, which the pilot is supposed to feel. The pilot controls the command model and no longer directly the helicopter. In general any dynamic model imaginable can be used as command model. But there are physical limits: the more the command model differs from the kinematics of the real helicopter the harder it gets to obtain a good model following performance. Thus the goal of the command model design is to create a model that is as easy to follow as possible (depending on the real aircraft kinematics) and that fulfills level 1 handling qualities criteria defined by the ADS-33.

The general structure of the command model consists of the model equation  $\dot{x} = \mathbf{A} \cdot x + \mathbf{B} \cdot u + f(x)$  where  $f(x)$  denotes nonlinearities like gravitation and aircraft kinematics. The command model is mostly decoupled by using only the on-axis derivatives inside the dynamics matrix  $\mathbf{A}$  and the input matrix  $\mathbf{B}$ .

In a first approach the derivatives were taken from the ACT/FHS system identification process. The remaining cross-axis coupling results only from the nonlinearities  $f(x)$  and the TC (turn coordination). The command model is optimized using the Control Designer's Unified Interface (CONDUIT<sup>®</sup>) with the ADS-33 criteria [26, 27, 28].

An example of an optimization result for the yaw axis is shown in Figure 18. The yaw bandwidth before the optimization was level 3 for the rate command (RC) model (small yellow triangle pointing upward) whereas that of the nonoptimized attitude command (AC) model (small green downwards pointing triangle) was level 2. After the optimization both bandwidth parameters could be moved well into level 1 (the big triangles).

The command model will encompass different command and hold functions, which can be chosen for the different axes independently. This allows for maximum flexibility in the tuning of the closed-loop behavior of the aircraft (mostly necessary for academic reasons). The various command model command types are: Rate Command (RC), Attitude Command (AC), Translational Rate Command (TRC), Acceleration Command (AcC), Rate of Climb Command (RocC), and Slope Command (SC). These command model types can be combined with various hold functions, which are: Attitude Hold (AH), Attitude Leveling (AL), Position Hold (PH), Airspeed Hold (AsH), Groundspeed Hold (GsH), Directional Hold (DH), and Height Hold (HH). Additionally, a Turn Coordination (TC) module according to [29] takes the effort of coordinating turns from the pilot and allows for smooth and comfortable flying. In Table 2 the different command and hold functions for each control axis are shown.

Thus different modes for different mission profiles can be chosen and analyzed. The states and their time derivatives generated by the command model are then fed to the feedforward controller.

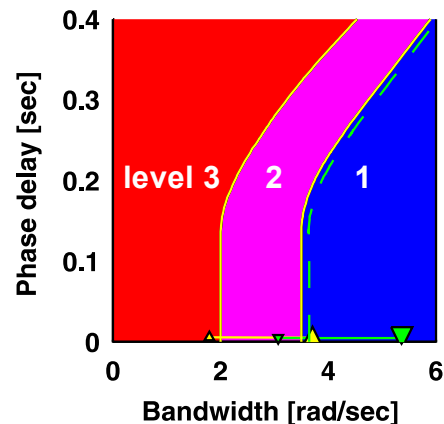


Figure 18. Bandwidth in yaw for RC (yellow upward pointing triangle) and AC (green downward pointing triangle) models before (small triangle) and after (big triangle) optimization

**Table 2. Possible command modes for the different control axes**

Pitch	Roll	Yaw	Collective
RCAH	RCAH	RCDH	Direct
ACAH	ARCAL	TC	RocCHH
TRCPH	ACAH		SCHH
AcCAsh	TRCPH		
AcCGsH			

### 7.3 Feedforward controller

The feedforward controller is designed to cancel the actual helicopter dynamics and to impose the desired command model dynamics on the ACT/FHS. In this way the design requirements of the feedback control branch can be separated into robustness and disturbance rejection, while leaving reference tracking to the feedforward controller. In ALLFlight identified linear state space models for different velocities are inverted for feedforward control [30, 31]. The identified models are transformed to avoid the collective rate input ( $\dot{\delta}_0$ ).

For a classical helicopter with four controls a maximum of four independent output variables can be selected to have exact model following behavior. Here, the feedforward controller is designed to provide model following for the commanded rates  $p$ ,  $q$ ,  $r$  and the vertical velocity in the helicopter coordinate system  $w$  and their derivatives.

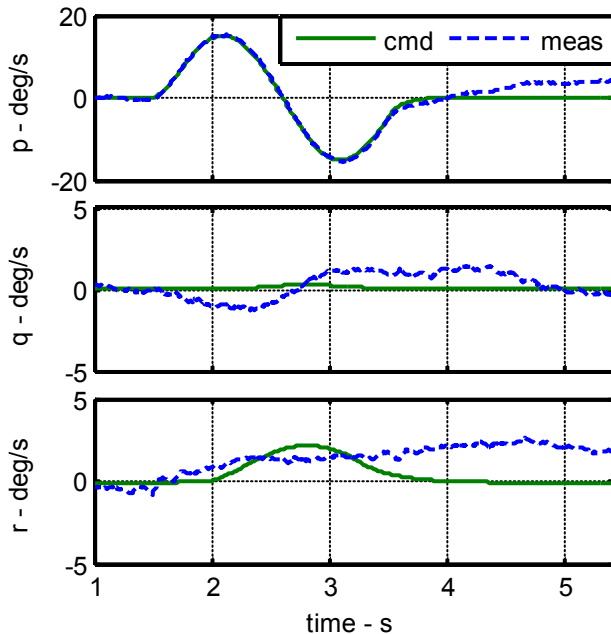


**Figure 19. Feedforward rate command with turn coordination roll maneuver**

The feedforward controllers were validated during a flight test campaign in 2011. During these tests the command model generated a decoupled rate command with turn coordination, when the

helicopter was stabilized at the defined trim velocity in forward flight or hover. In this way the decoupling capabilities of the feedforward controller without feedback were analyzed. In Figure 19 the commanded and measured rates during a roll maneuver are shown.

The feedforward controller shows good performance for pitch and roll commands on all axes from hover to 120 kts. Strong nonlinear effects of the Fenestron tail rotor are not addressed in linear models and therefore they cannot be compensated by a feedforward controller based on these linear models. The assessment of the feedforward decoupling performance is used in future work to identify missing terms (e.g. cross-axis coupling or engine model derivatives) of the linear model.

### 7.4 Feedback Controller

The feedback controller is used to compensate differences between commanded and measured values due to disturbances and inverse model deficiencies. The feedback controller is designed as a decoupled cascade structure for the cyclic axes and as single PI controller for the yaw and heave axes:

- Longitudinal cyclic  $\delta_x$ : two PI controllers for  $\theta$  and  $q$  in cascade
- Lateral cyclic  $\delta_y$ : two PI controllers for  $\phi$  and  $p$  in cascade
- Pedal  $\delta_p$ : PI controller for  $r$
- Collective  $\delta_0$ : PI controller for  $v_{down}$

A further dipole canceling controller suppresses air resonance mode oscillations [32], while the excitation of structural modes is prevented by dedicated band-stop filters.

Flight tests in 2011 showed the performance of the full model based control system in hover and forward flight in high dynamic and long-term maneuvers. In Figure 20 an extract of a piloted long term turn maneuver is depicted. The performance for all axes is good, the error between commanded and measured states is regarded as insignificant.

Further model based control flight tests will be conducted to show overall performance in the frequency domain via sweeps. In addition, the velocity-dependent inverse models are interpolated to arrive at a feedforward controller blending system. It is expected that this feedforward system will achieve higher control accuracy in the entire range of operating velocities.

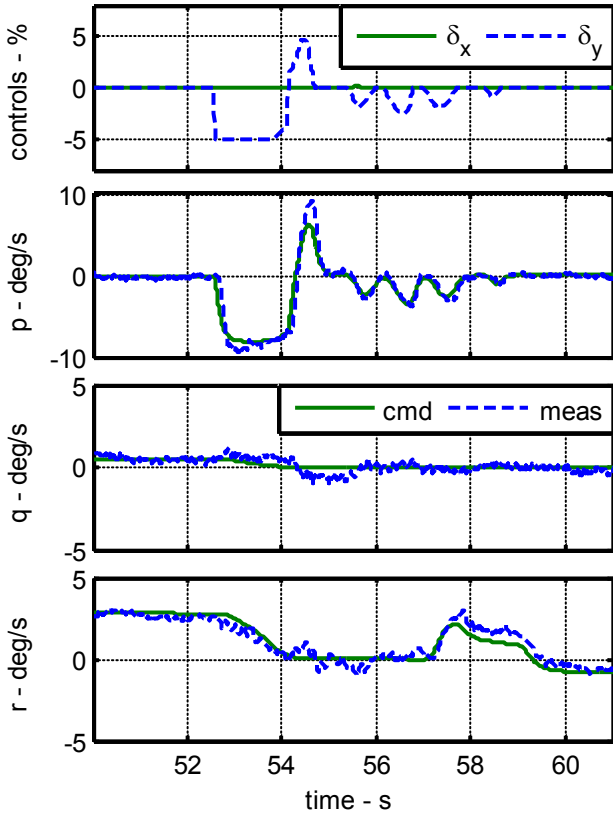


**Figure 20. Full MBC rate command with turn coordination roll maneuver**

## 8 ACTIVE INCEPTORS

The ACT/FHS has been equipped with two active sidesticks [33], a Stirling Dynamics Inc. Goldstick for the right hand (cyclic control) in 2006 and one from Liebherr Aerospace GmbH for the left hand (collective and optional yaw control) in 2009. They complete the man-machine interface by their ability to provide intuitive pilot cues through haptic perception. Equipped with electric motors the active sidesticks can generate forces up to 75 N, respectively 170 N depending on the type. The active sidestick can mimic second-order dynamics and generate additional nonlinear force effects. Its linear model parameters spring, mass, and damper, but also nonlinear friction, breakouts, soft and hard stops, and others can be modified online through a digital interface.

Within ALLFlight the sidesticks are used to fulfill two purposes. The first goal is the adaptation of the global force-feel dynamics (Flight Control Mechanical Characteristics – FCMC) to different response types of the controlled helicopter in order to optimize the handling qualities. The second goal is to use haptic cues and warnings in order to design envelope protections. These protections assist the helicopter pilot in avoiding to exceed structural limits and to fly into obstacles or terrain.

The FCMC of the active sidesticks are influenced by their equivalent model parameters, like stiffness (K), damping ratio (D), and eigenfrequency  $\omega_s$ . It is possible to find the optimum by iterative modification and evaluation based on quality measures like qualitative pilot feedback or standardized methods like Cooper-Harper rating (CHR). It is further possible to evaluate the parameter influence on quantitative measures, which appraise the quality level of fulfilling a task, e.g. handling quality levels or root mean square (RMS) of the error between task and result. This method is time consuming due to the necessity of flight trials in reality or simulation. To avoid this the idea came up to find a purely mathematical way, which should calculate the optimal stick dynamics, given only the controlled helicopter dynamics, as described in [34].

The effect of inceptor force-feel characteristics on piloted handling qualities has already been investigated in flight tests. The results of the ACT/FHS and the RASCAL flight tests are described in [35] and [36].

The transmission torque protection is a classical (but nonetheless very important) use case for haptic limit cueing. Several institutions used this protection to demonstrate the benefits of tactile cueing, as for example [37]. The transmission torque is mainly influenced by the collective lever position  $\delta_0$ . The purpose of a haptic limit protection is to cue the pilot at a position where he just does not exceed the limit. In some cases, like for the torque limitation, a predictor for the limiting parameter is required due to the high dynamics of the engine torque. A simple prediction can be made using a linear polynomial, considering  $\delta_0$  and pedal position  $\delta_p$ .

$$Q_{pred} = a\delta_0 + b\delta_p + c.$$

The parameters a, b, and c were identified offline from ACT/FHS flight test data, leading to a good estimate of the quasi-steady torque. As the considered limit is proportional to the collective lever position, the cueing algorithm reads:

$$\delta_{0,lim} = \delta_0 + \frac{1}{a}(Q_{lim} - Q_{pred}),$$

where the control reserve as distance between lever position and cue position is calculated from the reserve of the predicted transmission torque and its current limit. The proportionality factor is taken from the prediction polynomial. In order to compensate model uncertainties a low-pass error compensator was used according to [37].

Figure 21 shows some results from the first flight test of the haptic torque protection with the ACT/FHS. The first row shows the plots of the

collective lever position  $\delta_0$  and the position of the soft stop cue  $\delta_{0,lim}$ . The lower row shows the torque sensor value and the chosen torque limit  $Q_{lim}$ . It was set to 68% to have some margin against the real EC135 maximum takeoff power limit of 78%.

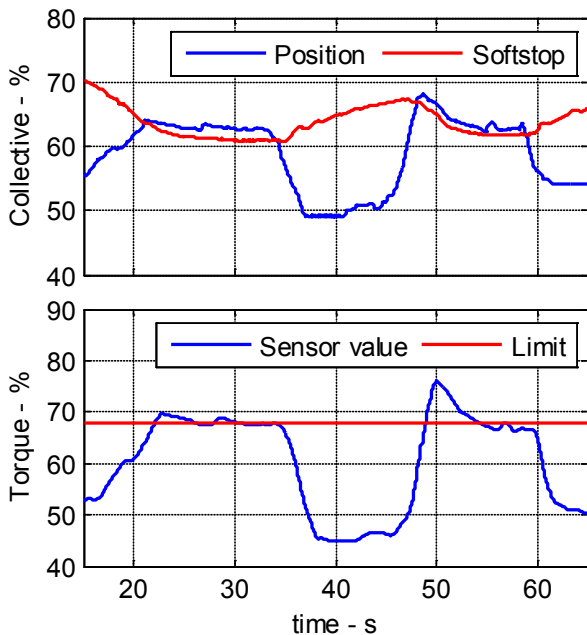


**Figure 21. Data from first flight of torque protection**

The collective controller position remains below or on the soft stop position. The torque remains below the set limit, apart from an overshoot at 50 s, after a harsh collective step input. Pilots commented that the haptic cue helps well to maintain the torque just below the limit. But they stated also that the transient overshoot of the torque after approaching the limit cue was too high. The reason for that was a too low time constant of the first-order error compensation, which led to a too fast compensation of the torque transient. The predictor was modified and will be tested in upcoming flight tests.

## 9 HMD - HELMET MOUNTED DISPLAY

Recently, DLR has integrated a wide field of view ( $80^\circ \times 40^\circ$ ) binocular helmet mounted display system (JedEye) produced by Elbit (Israel) into both the ACT/FHS and the Generic Cockpit Simulator GECO. The GECO comprises a collimated vision system, to efficiently test HUD and HMD designs (see Figure 22).

The system offers the possibility to increase the situational awareness especially under degraded visual conditions by displaying an adequate symbol set. A variety of different video input formats (RS170, DVI) can be used to present the current situation around the helicopter. In order to provide a synthetic vision display on a helmet mounted system

it requires a very precise measurement of the line of sight in conformance with the head movements of the pilot. This requires minimal latency during the data processing. Processing stages include the measurement of the pilot head's attitude, the transmission to the onboard system, the generation of a synthetic vision image, and the display of the image on the helmet. If the latency is too high, a conformal symbol set cannot be guaranteed, resulting in an increasing irritation and possible sickness of the pilot.



**Figure 22. Simulator with the JedEye HMD**

During the next months, DLR will investigate a new 3D conformal symbol set especially for landing in a degraded visual environment. On the basis of fused sensor data, relevant information will be extracted by applying methods described in the sensor data fusion section. Different types of display layouts are presently evaluated with helicopter pilots based on flight performance measures and pilot questionnaires.

## 10 SUMMARY

The unique ALLFlight full scale pilot assistance test environment gives the opportunity to test the whole chain from sensors, via the data fusion and trajectory planning including active inceptors to modern flight control techniques. The goal is a useful assistance system, that considers the pilot's workload and does not shift the workload from flying the aircraft to operating complex systems.

The main next step consists in performing extensive flight tests to validate the function of each subsystem (sensor data fusion, trajectory planning, model based control, active inceptors and HMD/HDD). In the end the overall system will also be evaluated in real flight under realistic conditions and scenarios, including fully automatic flight of the ACT/FHS.

## 11 REFERENCES

1. Helicopter Association International: FIVE-YEAR COMPARATIVE U. S. CIVIL HELICOPTER SAFETY TRENDS. Through 4th Quarter. 1 January – 31 December, 2008-2004.
2. NTSB, "Accidents, Fatalities, and Rates, 1988 through 2007, for U.S. Air Carriers Operating Under 14 CFR 121, Scheduled and Nonscheduled Service (Airlines)"
3. EHEST (European Helicopter Safety Team), "EHEST Analysis of 2000-2005 European helicopter accidents", European Aviation Safety Agency, ISBN 978-92-9210-095-7.
4. Swenson, R., "AFRL develops partial solution to helicopter brownout", <http://www.eglin.af.mil/news/story.asp?id=123052402>, 2007.
5. "Flying blind in Iraq: U.S. helicopters navigate real desert storms", <http://www.popularmechanics.com/>, 2006.
6. N.N., "LandSafe® Aircraft Survivability System", <http://www.oads.com/programs/landsafe.html>, 2008.
7. Martin, C., "In the thick of it all - surviving the brownout", Aviation Aftermarket Defense Magazine, 2007.
8. Einthoven, P., Miller, D., "The HACT Vertical Controller", American Helicopter Society 58th Annual Forum, 11-13 May 2002, Montreal, Canada.
9. Einthoven, P., Miller, D., Nicholas, J., Margetich, S., "Tactile Cueing Experiments with a Three Axis Sidestick", American Helicopter Society 57th Annual Forum, 09-11 May 2001, Washington, DC, USA.
10. Fujizawa, B., Ivler, C., Tischler, M., Moralez, E., Braddom, S. "In-Flight Simulation Control Law Design and Validation for RASCAL", American Helicopter Society 66th Annual Forum, 11-13 May 2010, Phoenix, AZ, USA.
11. Fletcher, J., Lusardi, J., Mansur, M., Arteburn, D., Cherepinsky, I., Driscoll, J., et al., "UH-60M Upgrade Fly-By-Wire Flight Control Risk Reduction using the RASCAL JUH-60A In-Flight Simulator", American Helicopter Society 64th Annual Forum, 29 April - 1 May 2008, Montréal, Canada.
12. Lueken, T., Korn, B., "PAVE: A prototype of a helicopter pilot assistant system", 33rd European Rotorcraft Forum, 11-13 Sep. 2007, Kazan, Russia.
13. Chamberlain, L., Scherer, S., Singh, S. "Self-Aware Helicopters: Full-Scale Automated Landing and Obstacle Avoidance in Unmapped Environments", American Helicopter Society 67th Annual Forum, 3-5 May 2011, Virginia Beach, VA, USA.
14. Kaletka, J., Kurscheid, H., Butter, U., "FHS, the New Research Helicopter: Ready for Service", Journal of Aerospace Science and Technology, vol. 9(5), 456-467, 2005.
15. Preissner, J., "The influence of the atmosphere on passive radiometric measurements", AGARD Conference on Millimeter and Submillimeter Wave Propagation and Circuits, vol. 245, 1978.
16. Lüken, T., Peinecke, N., Doehler, H., "ALLFlight - A sensor based conformal 3D situational awareness display for a wide field of view helmet mounted display", 38th European Rotorcraft Forum, 4.-7. Sep. 2012, Amsterdam, Netherlands.
17. Goerzen, C., Kong, Z., Mettler, B., "A survey of motion planning algorithms from the perspective of autonomous UAV guidance", Journal of Intelligent Robot Systems, vol. 57(1-4), 65-100, 2010.
18. Lier, M., "Statistical Methods for Helicopter Preliminary Design and Sizing", 37th European Rotorcraft Forum, 13-15 Sep. 2011, Milano, Italy.
19. Greiser, S., Wolfram, J., Gestwa, M., "Classification of pilot requirements used for takeoff planning", 37th European Rotorcraft Forum, 13-15 Sep. 2011, Milano, Italy.
20. Sehgal, M., Gondal, I., Dooley, L., "Collateral missing value imputation: A new robust missing value estimation algorithm for microarray data", Bioinformatics, vol. 21(10), 2417-2423, 2005.
21. Troyanskaya, O., et al., "Missing value estimation methods for DNA microarrays", Bioinformatics, 17(6):520-525, 2001.
22. Dechter, R., Pearl, J., "Generalized best-first search strategies and the optimality of A\*", Journal of the Association for Computing Machinery, vol. 32, 505-536, 1985.
23. Koenig, S., Likhachev, M., "Improved fast replanning for robot navigation in unknown terrain", Proceedings of the IEEE International Conference on Robotics and Automation (ICRA), vol.1, 968-975, 2002.

24. Strohmaier, T., Lantzs, R., Greiser, S., "Assisted landing for helicopters in confined areas", 36th European Rotorcraft Forum, 07-09 Sep. 2010, Paris, France.
25. Seher-Weiss, S., von Grünhagen, W., "EC135 System Identification for Model Following Control and Turbulence Modeling", Proceedings of the 1st CEAS European Air and Space Conference 2007 (CEAS-2007-275), Page 2439-2447, 10-13 Sep. 2007, Berlin, Germany.
26. Tischler, M., et. al., "Control Law Design and Optimization for Rotorcraft Handling Qualities Criteria Using CONDUIT", American Helicopter Society 55th Annual Forum, 25.-27. May 1999, Montréal, Canada.
27. Tischler, M., et. al., "Handling-Qualities Optimization and Trade-offs in Rotorcraft Flight Control Design", Presented at the RAeS Rotorcraft Handling Qualities Conference, University of Liverpool, U.K., 4-6 Nov, 2008.
28. "ADS-33E-PRF, Aeronautical Design Standard, Performance Specification, Handling Qualities Requirements for Military Rotorcraft", 2000.
29. Chen, R., Jeske, J.A., "Kinematic Properties of the Helicopter in Coordinated Turns", NASA Technical Paper 1773, April 1981.
30. Rynaski, E.G., "Adaptive Multivariable Model-Following", Proc. Joint Automatic Control Conference, San Francisco, 1980.
31. Taghizad, A., Bouwer, G., "Evaluation of Helicopter Handling Qualities Improvements During a Steep Approach Using New Piloting Modes", American Helicopter Society 55th Annual Forum, 25-27 May 1999, Montréal, Canada.
32. Lantzs, R., Wolfram, J., Hamers, M., "Increasing Handling Qualities and Flight Control Performance using an Air Resonance Controller", American Helicopter Society 64th Annual Forum, 29 April - 1 May 2008, Montréal, Canada.
33. von Grünhagen, W., Müllhäuser, M., Abildgaard, M., Lantzs, R., "Active inceptors in FHS for pilot assistance systems", 36th European Rotorcraft Forum, 07-09 Sep. 2010, Paris, France.
34. Nonnenmacher, D., Müllhäuser, M., "Optimization of the equivalent mechanical characteristics of active sidesticks for piloting a controlled helicopter", CEAS Aeronautical Journal, Springer Verlag, ISSN: 1869-5582, vol. 2, 2011.
35. von Grünhagen, W., Schönenberg, T., Lantzs, R., Lusardi, J., Fischer, H., Lee, D., "Handling qualities studies into the interaction between active sidestick parameters and helicopter response types", 38th European Rotorcraft Forum, 4.-7. Sep. 2012, Amsterdam, Netherlands.
36. Lusardi, J., Blanken, C., Ott, C., Malpica, C., von Grünhagen, W., "In Flight Evaluation of Active Inceptor Force-Feel Characteristics and Handling Qualities", American Helicopter Society 68th Annual Forum, 1.-3. May 2012, Fort Worth, USA.
37. Sahani, N., Horn, J., "Collective Axis Cueing and Limit Avoidance Algorithms for Carefree Maneuvering", American Helicopter Society Flight Controls and Crew System Design Specialists' Meeting, 2002, Philadelphia, USA.